Journal of Applied Polymer Science

Morphology and mechanical properties of natural rubber latex films modified by exfoliated Na-montmorillonite/polyethyleneimine-*g*-poly (methyl methacrylate) nanocomposites

Shuyi Wang, Xiaohui Tian, Jinyu Sun, Jin Liu, Junchao Duan

Shanghai Key Laboratory of Advanced Polymeric Materials, School of Materials Science and Engineering, East China University of Science and Technology, Shanghai 200237, People's Republic of China

Correspondence to: X. Tian (E-mail: tianxh@263.net)

ABSTRACT: Na-montmorillonite/polyethyleneimine-*g*-poly(methyl methacrylate) (Na-MMT/PEI-*g*-PMMA) nanocomposite latexes were prepared by soap-free emulsion polymerization in the aqueous suspension of Na-MMT. The exfoliated morphology of the nanocomposites was confirmed by XRD and TEM. With the aim of improving morphology and mechanical properties of natural rubber latex (NRL) films, the synthesized Na-MMT/PEI-*g*-PMMA nanocomposites were mixed with NRL by latex compounding technology. The results of SEM and AFM analysis showed that the surface of NRL/Na-MMT/PEI-*g*-PMMA film was smoother and denser than that of pristine NRL film while Na-MMT was dispersed uniformly on the fracture surface of the modified films, which suggested the good compatibility between NRL and Na-MMT/PEI-*g*-PMMA. The tensile strength of NRL/Na-MMT/PEI-*g*-PMMA films was increased greatly by 85% with 10 phr Na-MMT/PEI-*g*-PMMA when Na-MMT content was 3 wt % and the elongation at break also increased from 930% to 1073% at the same time. © 2016 Wiley Periodicals, Inc. J. Appl. Polym. Sci. **2016**, *133*, 43961.

KEYWORDS: clay; emulsion; films; mechanical properties; rubber

Received 7 January 2016; accepted 22 May 2016
DOI: 10.1002/app.43961

INTRODUCTION

Natural rubber latex (NRL), extracted from *Hevea brasiliensis* tree,[1] are widely used in manufacturing dipped products[2,3] such as medical gloves, balloons, and condoms due to its low cost, excellent elasticity, and film-forming property. However, the poor tensile strength of unvulcanized NRL film is a serious defect and limits its application in certain areas.

Recently, natural rubber/montmorillonite (NR/MMT)[4,5] nanocomposites have drawn much attention in many academic and industrial researches since nylon 6/montmorillonite nanocomposites were successfully synthesized in 1992.[6,7] NR/MMT nanocomposites possess excellent mechanical properties,[8] thermal stability,[9] and outstanding barrier properties.[10] The surface of MMT is hydrophilic while NR is hydrophobic, resulting in incompatibility between MMT and NR. So the modification of MMT is necessary. In order to change the hydrophilicity of MMT, alkylammonium cations were always used to decrease the surface energy of MMT by cation exchange.[11] After modification with alkylammonium cations, the compatibility between MMT and NR was improved. Meanwhile, the interlayer distance of MMT was increased, which was beneficial to introduce polymer.[12,13]

In general, two structures of MMT are available: intercalated structure or exfoliated structure.[14–17] Exfoliated MMT is preferred to increase the mechanical properties of NR, which is attributed to the highly anisotropic nature of MMT layers. As Amarasiri *et al.* reported, low loadings of exfoliated MMT contribute to high reinforcement of tensile strength without sacrificing the elastic properties of NRL film.[18] *In situ* emulsion polymerization is an effective way to exfoliate MMT.[19–21] The introduction of alkylammonium cations may even provide functional groups which could initiate polymerization of monomers, rendering MMT exfoliated. MMT also shows a high aspect ratio and swelling capability which are helpful for the exfoliation. Choi *et al.* obtained exfoliated PMMA/MMT nanocomposites through soap-free emulsion polymerization using a reactive surfactant, 2-acrylamido-2-methyl-1-propanesulfonic acid, to modify MMT.[22]

The purpose of this work was to investigate the effects of Na-montmorillonite/polyethyleneimine-*g*-poly(methyl methacrylate) (Na-MMT/PEI-*g*-PMMA) nanocomposites on the morphology and mechanical properties of NRL films. Na-MMT/PEI-*g*-PMMA nanocomposite latexes were prepared by soap-free emulsion polymerization.[23,24] An amphipathic macromolecule PEI was introduced into the gallery of Na-MMT and formed

macroradicals to initiate the graft copolymerization of MMA in the interlayer of Na-MMT, which may contribute to the exfoliation of Na-MMT. It is important to note that the synthesis of Na-MMT/PEI-*g*-PMMA nanocomposites is rarely reported. Then, the synthesized nanocomposites were mixed with NRL *via* latex compounding. The surface morphologies and fracture surface morphologies of the modified NRL films were characterized by SEM and AFM. Mechanical properties of NRL/Na-MMT/PEI-*g*-PMMA films were also studied.

EXPERIMENTAL

Materials

Na-montmorillonite [Na-MMT; cationic exchange capacity (CEC) = 100 meq/100 g] was obtained from Zhejiang Fenghong new material Co. Ltd. NRL with a solid content of 60% (w/w) was supplied by Hainan American International Xianghe Industrial. Branched polyethyleneimine (PEI; molecular weight of 70 kDa; 50 wt % solution in water, amorphous state) and methyl methacrylate (MMA) were purchased from Aladdin. *tert*-Butyl hudroperoxide (TBHP, 70% solution in water) was obtained from Sinopharm Chemical Reagent Co. Ltd. MMA was purified by passing through a column packed with neutral and basic aluminum oxide adsorbents. PEI was diluted with deionized water to 10 wt % before subjected to polymerization. All other reagents used in this study were of analytical grade. Deionized water was used as the dispersion medium.

Synthesis of Na-MMT/PEI-*g*-PMMA Nanocomposites

A series of pristine Na-MMT (from 0 to 10 wt % of Na-MMT relative to weight of MMA monomer) dispersed in 85 g distilled water was added into a 250 mL four-neck glass flask. Ten grams of PEI aqueous solution was added dropwise to Na-MMT aqueous suspension and mechanically stirred at room temperature overnight.

The above solution was poured into a flask equipped with a magnetic stirrer, a reflux condenser, and a rubber septum. Then it was heated to 50 °C (±1 °C) under nitrogen atmosphere. Four grams of purified MMA monomer was added to PEI/Na-MMT aqueous. After stirring for 30 min, the mixture was heated to 80 °C (±1 °C). The polymerization started after adding 1 mL TBHP (10 m*M*) solution and was kept for 2 h. The synthesized Na-MMT/PEI-*g*-PMMA nanocomposites latex containing 1 wt % Na-MMT was designated as 1%Na-MMT/PEI-*g*-PMMA latex and so on. The obtained latexes were purified by repeated centrifugation (10,000 rpm, 30 min), decantation, and redispersion for three times to remove the unreacted PEI until the conductivity of the supernatant was equal to the water. Furthermore, they were purified by Soxhlet extraction with chloroform for 48 h after desiccation. The solids content of the latex was determined by a gravimetric method, based on the weight of the latex and its dry weight. The MMA conversion and grafting efficiency of MMA to PEI were calculated as follows:

$$\%\ \text{solids content} = \frac{\text{weight of dried latex}}{\text{weight of latex}} \times 100 \quad (1)$$

$$\%\ \text{conversion} = \frac{\text{weight of dried latex} - \text{weight of PEI} - \text{weight of Na-MMT}}{\text{weight of monomer feed}} \times 100 \quad (2)$$

$$\%\ \text{grafting efficiency} = \frac{\text{weight of grafted PMMA}}{\text{weight of the total polymerized MMA}} \times 100 \quad (3)$$

Preparation of Latex Films

Latex blends were obtained by mixing certain proportions of the two latexes (NRL and Na-MMT/PEI-*g*-PMMA latex with known solids contents). Na-MMT/PEI-*g*-PMMA latex was sonicated for 10 min and the pH was adjusted to 9 to 10 with ammonium hydroxide before mixed with NRL. NRL/Na-MMT/PEI-*g*-PMMA latexes were produced by adding different proportions of Na-MMT/PEI-*g*-PMMA [5 parts per hundred parts rubber (phr), 10 phr, 15 phr, or 20 phr] based on the dry rubber content. The total solids content of the blends was adjusted with deionized water to 20 wt %. Latex blends were stirred for 2 h before using. Then they were poured into PS plates and dried at 60 °C for 12 h after standing for 6 h.

Characterization

Fourier transform-infrared spectroscopy (FT-IR; Nicolet 6700) was used to identify the chemical structure of Na-MMT/PEI-*g*-PMMA nanoparticles. The scanning range for each spectrum was between 4000 cm^{-1} and 400 cm^{-1} with 4 cm^{-1} resolution at 16 scans. Na-MMT/PEI-*g*-PMMA was isolated by Soxhlet extraction with chloroform to remove the homopolymer of PMMA[23] before taking FT-IR measurement.

The T_g values of PEI, PMMA and the graft copolymers PEI-*g*-PMMA were characterized using a DSC8500(DSC8500, Perkin-Elmer) under N_2 atmosphere at a heating rate of 10 °C /min from −50 °C to 150 °C.

X-ray diffractograms (XRD) were obtained from a D/max 2550V X-ray diffraction analyzer using Cu-Kα radiation (λ = 0.1542 nm) and were recorded between 0.7° and 10° with diffraction angle 2θ at 2°/min. The operating current and the voltage were 200 mA and 40 kV, respectively.

The morphologies of Na-MMT/PEI-*g*-PMMA nanocomposites, NRL particles, NRL/PEI-*g*-PMMA particles, and NRL/Na-MMT/PEI-*g*-PMMA nanocomposites were determined with a JEM 1400 transmission electron microscope (TEM). Each sample was prepared by wetting a carbon-coated grid with a small drop of the dilute particle dispersion.

Scanning electron microscope (SEM, S-4800, Hitachi) was used to examine the surface and fracture surface morphologies of the films. A small piece of the film was placed flatly on the sample stage with conductive adhesive. The film was sputter-coated for 30 s under vacuum with a thin layer of nanogold before observation at scanning voltage of 5 kV.

The films were imaged with Veeco/DI atomic force microscopy (AFM) operating in the tapping mode. Representative scans of the film surface (each at 20 × 20 μm^2) at three different locations were obtained for each sample. AFM images were

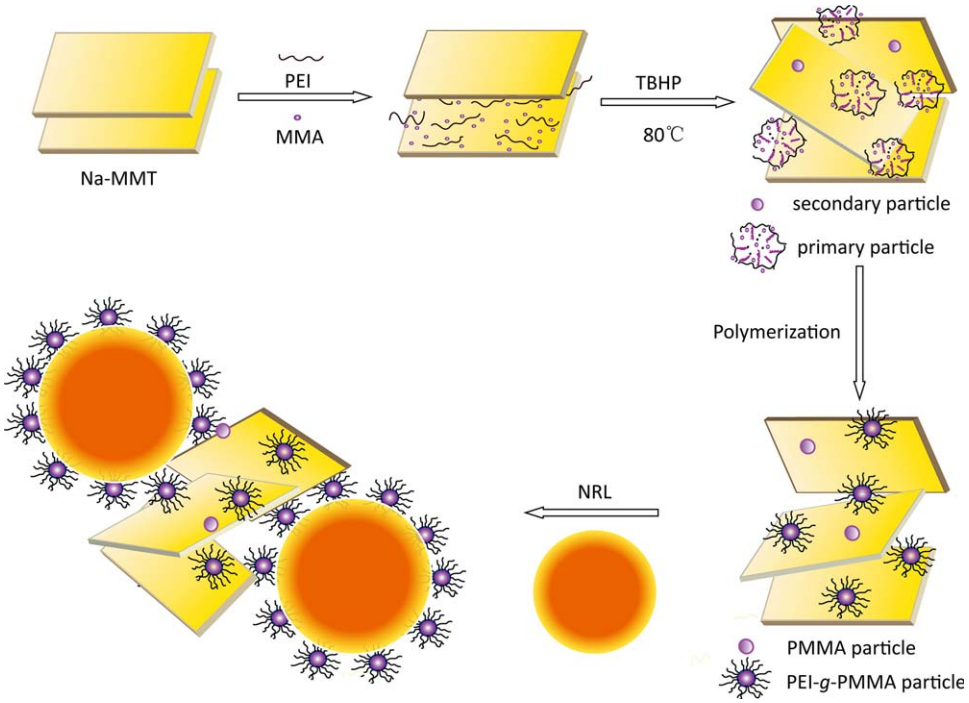

Figure 1. Proposed mechanism of exfoliated Na-MMT/PEI-*g*-PMMA nanocomposites prepared via soap-free emulsion polymerization process and mixed with NRL. [Color figure can be viewed in the online issue, which is available at wileyonlinelibrary.com.]

presented to describe the morphology of film surface. To monitor the change in morphology of the films with different Na-MMT/PEI-*g*-PMMA latex contents, the surface mean roughness was recorded.

Tensile property tests were operated according to GB 7543-2006. Five dumb bell test pieces with 50.0 mm long and 4.0 mm wide rectangular working sections were cut from each blending film which thickness have been measured by a micrometer gauge. The elongation at break and tensile strength of the samples were measured by universal test tension machine (CMT2202) and pilled at a rate of 400.0 mm/min.

RESULTS AND DISCUSSION

Proposed Mechanism for the formation of NRL/Na-MMT/PEI-*g*-PMMA Nanocomposites

The MMA conversion for PEI-*g*-PMMA latex and 3%Na-MMT/PEI-*g*-PMMA latex were 82% and 78%, respectively. And the grafting efficiency of MMA to PEI for PEI-*g*-PMMA latex and 3%Na-MMT/PEI-*g*-PMMA latex were 47% and 45%, respectively. The formation mechanism of NRL/Na-MMT/PEI-*g*-PMMA nanocomposites was proposed in Figure 1. In the first step, PEI entered into the gallery of Na-MMT and the surface of Na-MMT became hydrophobic. The amino groups on PEI could be protonated in water and made it possible to conduct cationic exchange with sodium ions on Na-MMT. In the second step, the TBHP initiator interacted with amine groups on the PEI backbone, forming redox pairs. The macroradicals generated by PEI were used to initiate the polymerization of MMA in the gallery of Na-MMT.[25] As the oligoradicals of PMMA were too long to dissolve in water, they precipitated to form the primary particles, where PEI became the shell around the PMMA particles and acted as electrostatic stabilizers.[26] In the next step, more and more MMA monomers entered into the gallery of Na-MMT to form PEI-*g*-PMMA particles, which triggered the exfoliation of Na-MMT.[27] However, the radicals from TBHP could also initiate the homopolymerization of MMA directly to generate the secondary PMMA particles in Na-MMT interlayer. After latex compounding, the synthesized Na-MMT/PEI-*g*-PMMA nanocomposites were fixed around NRL particles through physicochemical interactions.

Characterization of Na-MMT/PEI-*g*-PMMA Nanocomposites

Figure 2 shows FT-IR spectra of Na-MMT/PEI-*g*-PMMA nanocomposites compared to those of Na-MMT and original PEI polymers. The spectrum of Na-MMT [Figure 2(a)] showed that O-H stretching vibration peak was at 3624 cm^{-1}, while Si-O stretching vibration was appeared at 1089 cm^{-1} and Si-O-Si at 1038 cm^{-1}. The FT-IR spectrum of PEI polymer [Figure 2(b)] displayed the characteristic signals at 2932 cm^{-1} (asymmetric stretching of CH_2), 2849 cm^{-1} (symmetric stretching of CH_2), 1651 cm^{-1} (N-H deformation vibration of NH_2) and 1601 cm^{-1} (N-H deformation vibration of NH^{3+}). Figure 2(c) shows the spectrum of Na-MMT/PEI-*g*-PMMA. A strong peak at 1731 cm^{-1} corresponding to C=O stretching vibration proved the existence of grafted PMMA onto PEI. Moreover, the N-H deformation vibration of PEI shifted from 1651 cm^{-1} to 1641 cm^{-1} and the out-of-plane Si-O stretching vibration of Na-MMT moved to 1039 cm^{-1}, which may be caused by the electrostatic interaction and hydrogen-bond between Na-MMT and PEI.

Furthermore, DSC is applied to characterize the glass transition temperature (T_g) of materials. Figure 3 displayed the DSC

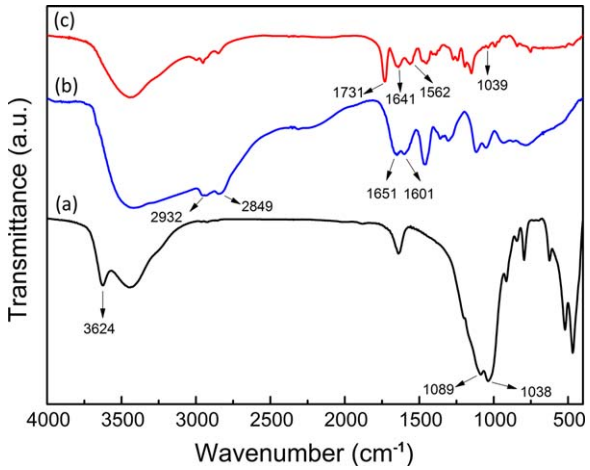

Figure 2. FT-IR spectra of (a) Na-MMT, (b) PEI, (c) Na-MMT/PEI-*g*-PMMA nanocomposites. [Color figure can be viewed in the online issue, which is available at wileyonlinelibrary.com.]

curves of pure PEI, PMMA, and PEI-*g*-PMMA. The T_g observed for PMMA was 117.35 °C and PEI was −14.72 °C, respectively. It could be seen that PEI-*g*-PMMA showed a single T_g at 46.93 °C between the T_g of PMMA and PEI which indicated that PMMA was incorporated into PEI main chains.

Figure 4(a) shows that the XRD diffraction peak of Na-MMT is at $2\theta = 7.0°$, which reveals a symmetric diffraction peak with $d_{001} = 1.26$ nm according to the equation $2d\sin\theta = n\lambda$. Once Na^+ in the gallery of Na-MMT was replaced by PEI, the diffraction peak of Na-MMT/PEI [Figure 4(b)] was shifted to 6.3° obviously, indicating that an intercalated structure was formed and the interlayer spacing of d_{001} increased from 1.26 nm to 1.40 nm, which would be helpful for the polymerization in Na-MMT gallery.[14] Figure 4(c–f) shows the XRD patterns of a series of Na-MMT/PEI-*g*-PMMA nanocomposites with different addition amounts of Na-MMT after soap-free emulsion polymerization. The peak at $2\theta = 6.3°$ was almost disappeared when the addition amounts of Na-MMT was up to 3 wt % weight

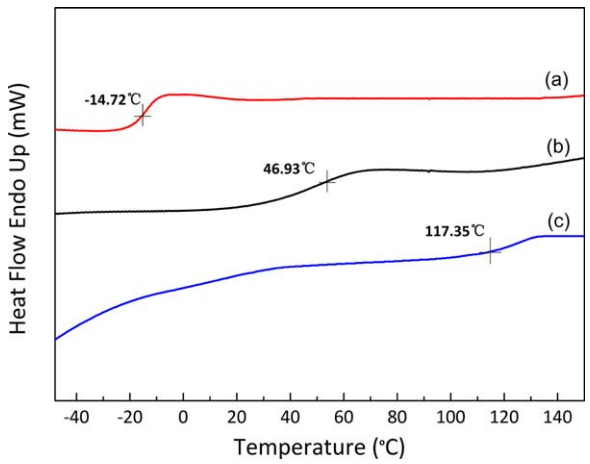

Figure 3. DSC curves of (a) PEI, (b) PEI-*g*-PMMA, and (c) PMMA polymers. [Color figure can be viewed in the online issue, which is available at wileyonlinelibrary.com.]

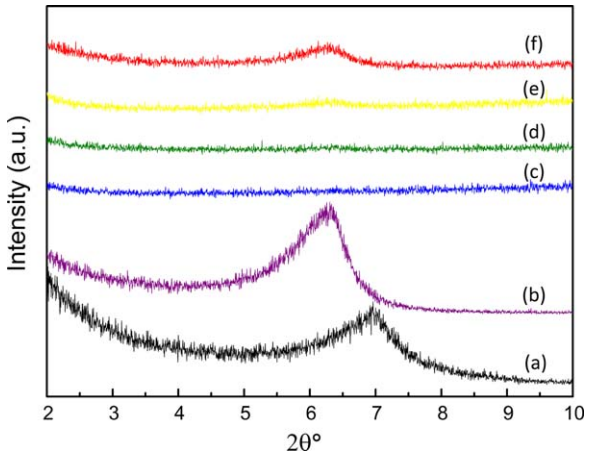

Figure 4. X-ray diffraction patterns of (a) Na-MMT, (b) Na-MMT/PEI, (c) 1%Na-MMT/PEI-*g*-PMMA, (d) 3%Na-MMT/PEI-*g*-PMMA, (e) 5%Na-MMT/PEI-*g*-PMMA, (f) 10%Na-MMT/PEI-*g*-PMMA powder samples. [Color figure can be viewed in the online issue, which is available at wileyonlinelibrary.com.]

ratio of MMA monomer as shown in Figure 4(c). It could be confirmed that Na-MMT platelets were well exfoliated by PEI-*g*-PMMA particles, which was consistent with TEM image [Figure 5(a)]. Nevertheless, once the addition amounts of Na-MMT were up to 5 wt % and 10 wt %, a weak peak appeared again at $2\theta = 6.3°$, which suggested that Na-MMT slices were intercalated or exfoliated incompletely. In the following, we only chose 3%Na-MMT/PEI-*g*-PMMA for discussion. Because Na-MMT in this content was completely exfoliated which contributed to the maximum interactions with NRL. In fact, it is generally accepted that exfoliated systems give better properties than intercalated ones.[28]

Figure 5(a) displays the morphologies of 3%Na-MMT/PEI-*g*-PMMA particles. The dark lines were corresponded to the silicate layers where many PEI-*g*-PMMA particles were embedded conspicuously and contributed to exfoliate the Na-MMT slices. The particle sizes of PEI-*g*-PMMA around 80 to 100 nm were measured from TEM image based on the images of dozens of particles. Many Na-MMT/PEI-*g*-PMMA particles aggregated together which may due to that some exfoliated Na-MMT were embedded or surrounded by the same PEI-*g*-PMMA particles. From Figure 5(b), a single Na-MMT/PEI-*g*-PMMA particle was observed in red circle where a slice of Na-MMT was inserted in the middle of two PEI-*g*-PMMA particles. The particle size of PEI-*g*-PMMA was around 80 nm and the length of Na-MMT was about 50 nm.

The Morphology of Latexes and Films

The microstructures of NRL, NRL/PEI-*g*-PMMA and NRL/3%Na-MMT/PEI-*g*-PMMA latexes were observed by TEM in Figure 6. NRL particles possessed a hydrophobic core of polyisoprene which was surrounded by a mixed layer of proteins and phospholipids [Figure 6(a)]. NRL particles were polydispersity and the diameters of the particles were about 500 to 1000 nm unevenly.[1] Figure 6(b) shows the morphology of NRL/PEI-*g*-PMMA latex. The diameters of the PEI-*g*-PMMA particles were around 130 nm measured from TEM images. After blended

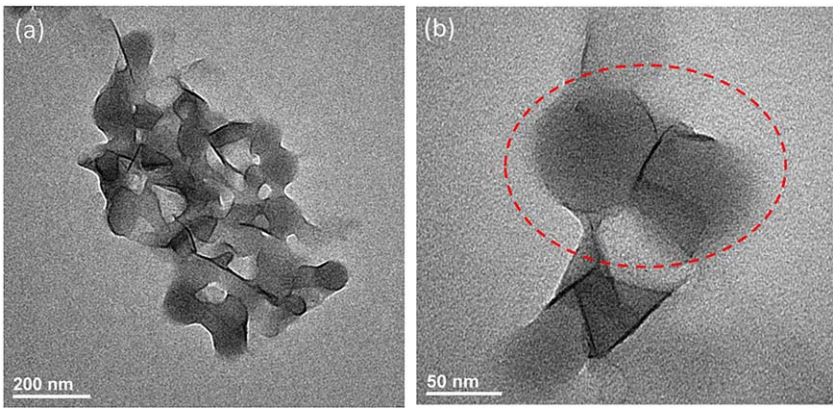

Figure 5. TEM images of 3%Na-MMT/PEI-*g*-PMMA. (a) Lots of Na-MMT/PEI-*g*-PMMA particles, (b) a single Na-MMT/PEI-*g*-PMMA particle. [Color figure can be viewed in the online issue, which is available at wileyonlinelibrary.com.]

with NRL latex, a certain amount of PEI-*g*-PMMA particles were absorbed onto NRL particles. Figure 6(c) reveals that the exfoliated Na-MMT slice is attached to NRL particles tightly due to the connection of PEI-*g*-PMMA particles which surround the NRL particles. The diameters of PEI-*g*-PMMA particles embedded into the Na-MMT slice were about 80 to 100 nm, smaller than that of PEI-*g*-PMMA particles in Figure 6(b), which is because Na-MMT is free-radical scavengers and traps.[29] The minerals in Na-MMT inhibit the free radical reactions by absorption of the propagating particles and then the radicals undergo bimolecular termination.

SEM is employed to observe the surface and fracture surface morphologies of NRL films. Figure 7(a) shows that voids of different sizes are distributed randomly on the surface of pristine NRL film due to the existence of proteins and phospholipids which resist the deformation of rubber particles during the film formation process.[1] However, a flat and void-free film was obtained with the addition of PEI-*g*-PMMA to NRL [Figure 7(b)]. As Sunintaboon *et al.* reported, the long-chain fatty acid soaps and protein around rubber particles supply negative charges.[26] PEI-*g*-PMMA particles were positively charged which could combine with the protein/phospholipid shells of rubber particles by electrostatic interactions in the initial stage of film formation. After the close packing and fusion of rubber particles, PEI-*g*-PMMA chains would spread and get entangled with rubber chains. At last, PEI-*g*-PMMA chains would fill up the voids owning to the good film-forming property of PEI and result in a compact NRL film. Figure 7(c) also reveals a smooth surface of NRL/3%Na-MMT/PEI-*g*-PMMA film, which is similar to that of NRL/PEI-*g*-PMMA film. It was clear to see that no precipitation of Na-MMT displayed on the surface of the film, which suggested that the compatibility between NRL and Na-MMT was improved.

Figure 7(d–f) shows the fracture surface morphologies of pristine and modified NRL films. There were some voids existed in the pristine NRL film as shown in Figure 7(d). However, voids disappeared in NRL films after modified by PEI-*g*-PMMA and 3%Na-MMT/PEI-*g*-PMMA [Figure 7(d,e)]. Besides, plenty of white clusters around 1 to 2 μm were distributed on the fracture surface of NRL/3%Na-MMT/PEI-*g*-PMMA films without aggregation [Figure 7(f)]. The white cluster represented the exfoliated Na-MMT slice, while the gray background was the coalescence of NRL and PEI-*g*-PMMA particles. It could be confirmed that the exfoliated Na-MMT could be uniformly distributed throughout the NRL films during the film formation process.

AFM is another useful method to observe the surface morphologies of films. Figure 8 shows the AFM images of NRL films modified with different proportions of 3%Na-MMT/PEI-*g*-PMMA nanocomposites. The pristine NRL film [Figure 8(a)] could be discerned easily from the modified films based on

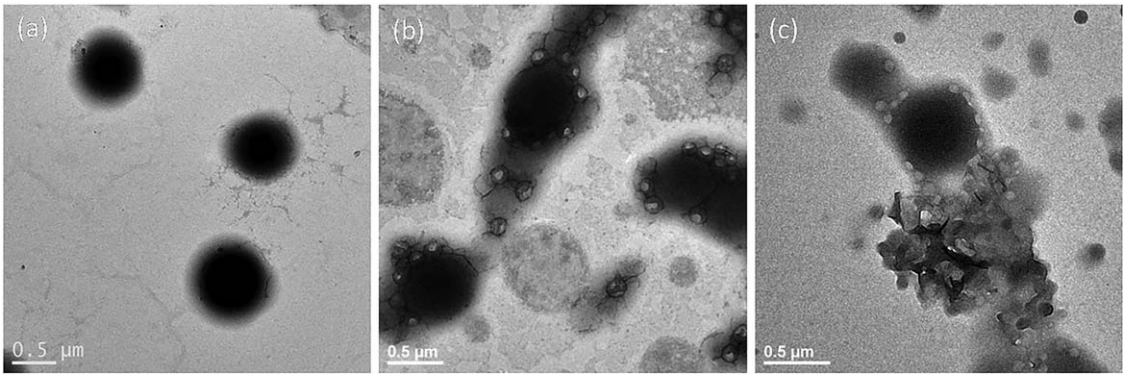

Figure 6. TEM images of (a) NRL particles, (b) NRL/PEI-*g*-PMMA particles, and (c) NRL/3%Na-MMT/PEI-*g*-PMMA nanocomposites.

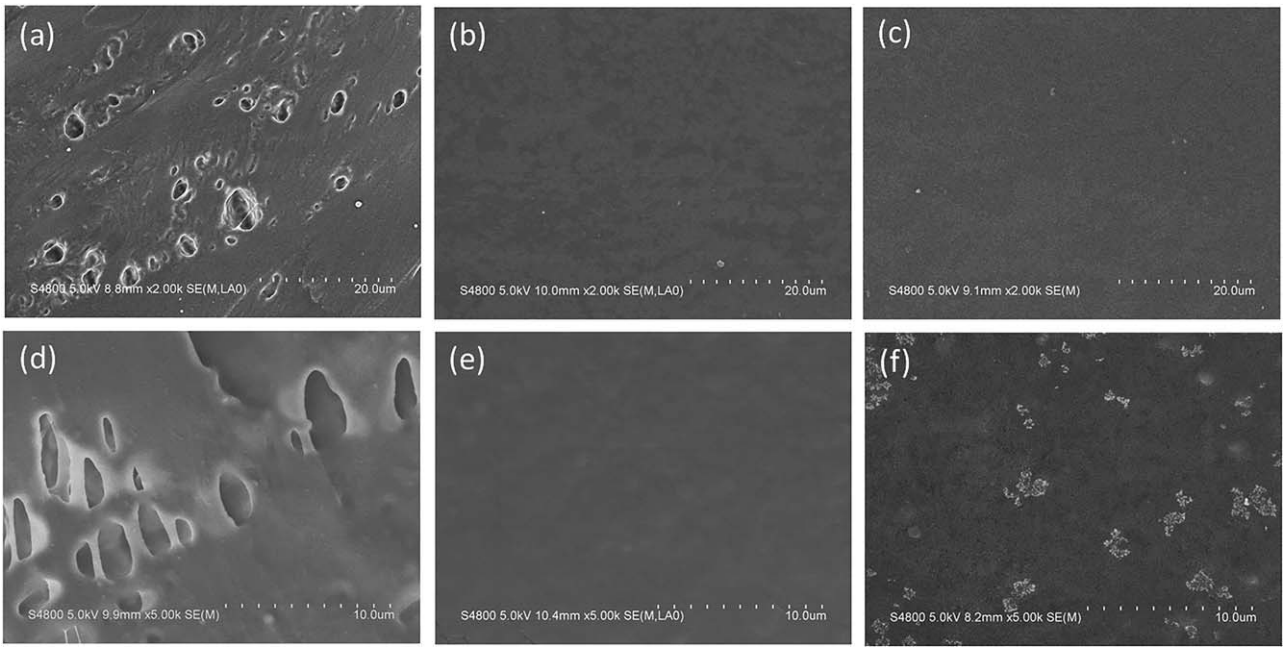

Figure 7. SEM micrographs of surface morphologies of (a) pristine NRL film, (b) NRL/PEI-*g*-PMMA film, (c) NRL/3%Na-MMT/PEI-*g*-PMMA film and the fracture surface morphologies of (d) pristine NRL film, (e) NRL/PEI-*g*-PMMA film, (f) NRL/3%Na-MMT/PEI-*g*-PMMA film.

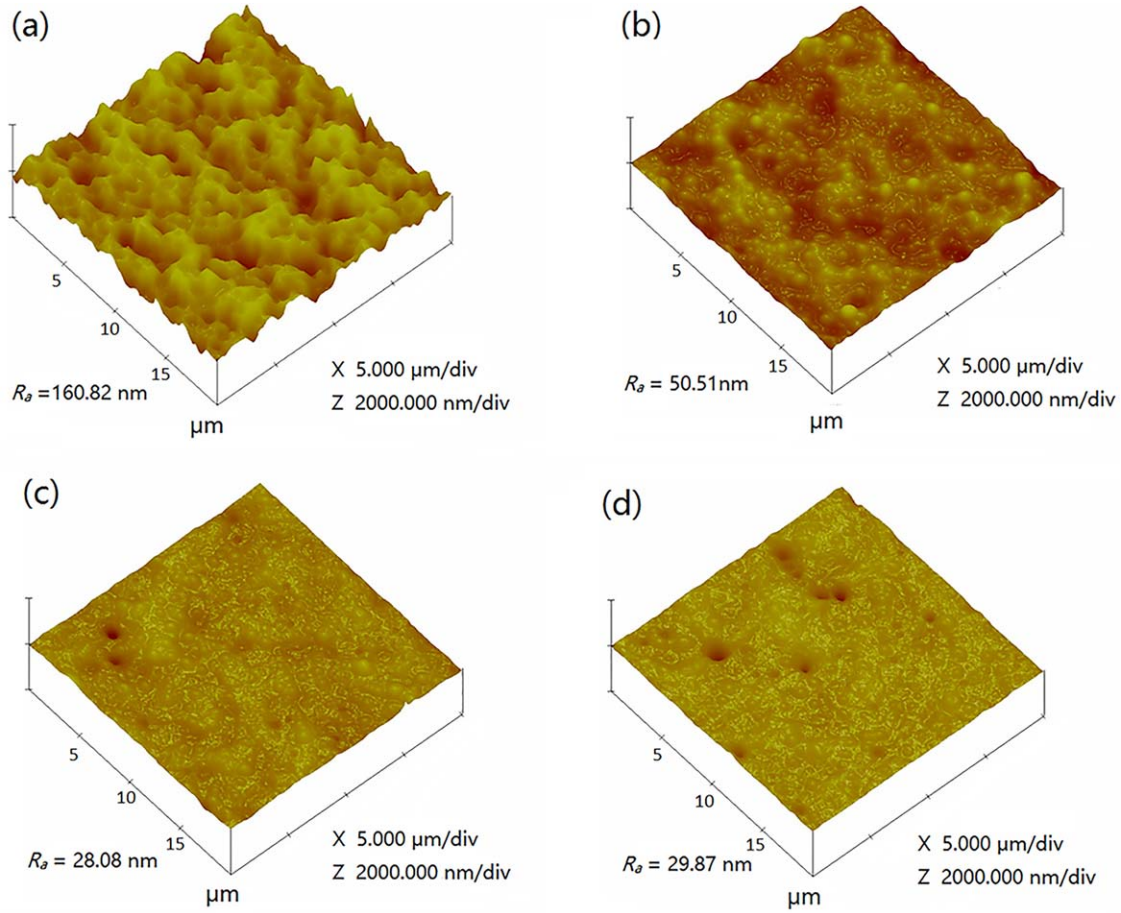

Figure 8. AFM images of NRL films blended with 3%Na-MMT/PEI-*g*-PMMA contents 1 day after preparation (scan size = 20 μm). The addition amounts of 3%Na-MMT/PEI-*g*-PMMA contents: (a) 0 phr; (b) 5 phr; (c) 10 phr; and (d) 15 phr. [Color figure can be viewed in the online issue, which is available at wileyonlinelibrary.com.]

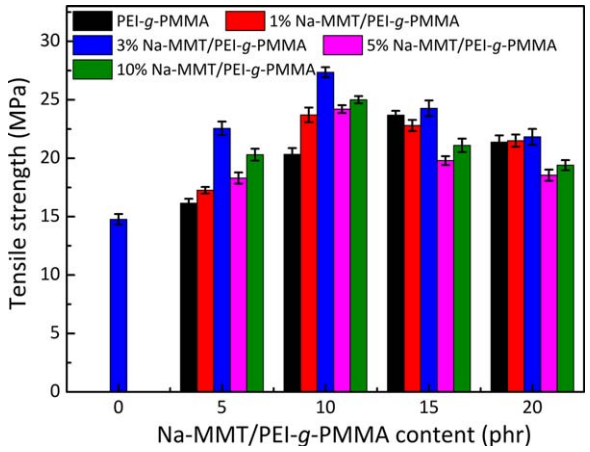

Figure 9. Tensile strength of NRL films modified by neat PEI-*g*-PMMA and Na-MMT/PEI-*g*-PMMA with different Na-MMT contents. [Color figure can be viewed in the online issue, which is available at wileyonlinelibrary.com.]

bumpy surface with vast sharp embossments that resulted from the accumulation of proteins and phospholipids.[1] When 5 phr 3%Na-MMT/PEI-*g*-PMMA latex was added to NRL, the surface morphology showed that the sharp embossments became gentle [Figure 8(b)]. It might result from the strong interaction between NRL and Na-MMT/PEI-*g*-PMMA particles, which prevented the rupture of protein and phospholipids from NRL particles, thus the surface mean roughness (R_a) of the film dropped to 50.51 nm drastically. After increasing the addition amounts of 3%Na-MMT/PEI-*g*-PMMA, we found that a smooth surface morphology of the modified NRL film was displayed as shown in Figure 8(c). The R_a of the modified film was only 28.08 nm when 10 phr 3%Na-MMT/PEI-*g*-PMMA was added to NRL. Na-MMT/PEI-*g*-PMMA nanocomoposites prevented the proteins and phospholipids of NRL from migrating to the surface of NRL films. The excess PEI-*g*-PMMA chains would also fill up the pits during the film formation process. Nevertheless, no distinct sign insured the trace of exfoliated Na-MMT slice on the surface of the modified NRL film which was consistent with the SEM results. Once the addition amounts of 3%Na-MMT/PEI-*g*-PMMA were increased to 15 phr, there was no obvious distinction on the surface morphology of the modified NRL films compared to Figure 8(c).

Mechanical Properties of NRL/PEI-*g*-PMMA and NRL/Na-MMT/PEI-*g*-PMMA Films

The mechanical properties of NRL films modified by neat PEI-*g*-PMMA and Na-MMT/PEI-*g*-PMMA with different Na-MMT contents are presented in Figures 9 and 10. The NRL/3%Na-MMT/PEI-*g*-PMMA films showed the most excellent tensile properties and we could conclude that a small amount of Na-MMT made great contributions to improving the tensile strength of NRL films.

The tensile strength of NRL/PEI-*g*-PMMA films without Na-MMT showed a growing trend from 14.78 MPa to 23.68 MPa which was increased by 60.22% when the addition amounts of PEI-*g*-PMMA were less than 15 phr. However, a higher amount of PEI-*g*-PMMA contents was no longer helpful to enhance the tensile strength of NRL films. For NRL/Na-MMT/PEI-*g*-PMMA nanocomposite films with different Na-MMT contents, the tensile strength showed a similar trend which increased first and then decreased. It should be noted that the tensile strength got to the maximum when the addition amounts of Na-MMT was up to 3 wt % in Na-MMT/PEI-*g*-PMMA nanocomposites. The maximum value of tensile strength was reached to 27.35 MPa, much higher than that of NRL/PEI-*g*-PMMA films when 10 phr 3%Na-MMT/PEI-*g*-PMMA was added to NRL. It proved that the addition of the exfoliated Na-MMT made significant reinforcing effects on increasing the tensile strength of the modified films. As Mathew *et al.*[30] reported, exfoliated Na-MMT oriented towards the strain direction during stretching,[18] which was conducive to the crystallization of rubber chains. Meanwhile, Na-MMT were dispersed uniformly in rubber matrix and acted as a physical crossing points (as shown in SEM), which reduced the slippage of rubber chains and resulted in the enhancement of tensile strength. For NRL/5%Na-MMT/PEI-*g*-PMMA and NRL/10%Na-MMT/PEI-*g*-PMMA films, the ultimate tensile strength was lower than that of NRL/3%Na-MMT/PEI-*g*-PMMA films. It may be caused by the incomplete exfoliation of Na-MMT, which resulted from the less interaction between NRL and Na-MMT/PEI-*g*-PMMA nanocomposites.

Figure 10 displays the elongation at break of NRL films modified by neat PEI-*g*-PMMA and Na-MMT/PEI-*g*-PMMA with different Na-MMT contents. For NRL/PEI-*g*-PMMA films, the elongation at break kept a relatively stable elasticity which seemed to be affected slightly with the increase of PEI-*g*-PMMA. NRL/3%Na-MMT/PEI-*g*-PMMA films showed the maximum elongation at break which was increased from 930% to 1073% when the addition amounts of Na-MMT/PEI-*g*-PMMA was 10 phr. It indicated that the well-dispersed Na-MMT nanoplatelets acted like a pin to stop the crack propagation when the films were stretched.[29] Nevertheless, when the addition amounts of Na-MMT were up to 5 wt % and 10 wt % in Na-MMT/PEI-*g*-PMMA, the elongation at break of NRL/Na-MMT/PEI-*g*-PMMA films decreased gradually with increasing the addition amounts of Na-MMT/PEI-*g*-PMMA. It could be ascribed to less interaction between NRL and incompletely

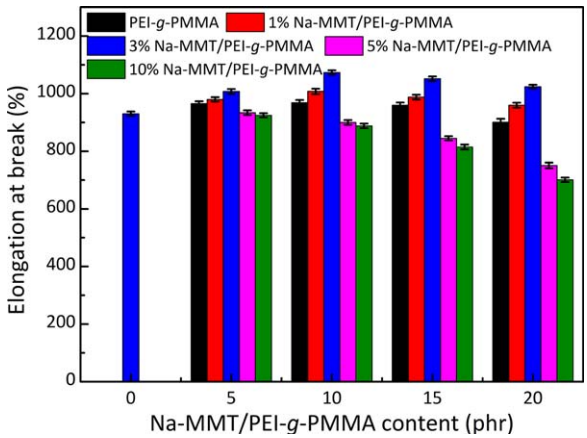

Figure 10. Elongation at break of NRL films modified by neat PEI-*g*-PMMA and Na-MMT/PEI-*g*-PMMA with different Na-MMT contents. [Color figure can be viewed in the online issue, which is available at wileyonlinelibrary.com.]

exfoliated Na-MMT. The restacking of excess Na-MMT nanoplatelets also made NRL film become more brittle.

CONCLUSIONS

To conclude, the exfoliated Na-MMT/PEI-*g*-PMMA nanocomposite latexes were synthesized via soap-free emulsion polymerization and then used to modify NRL films by latex compounding technology. The synthesis mechanism of exfoliated Na-MMT/PEI-*g*-PMMA nanocomposites and its interaction with NRL were studied. The NRL/Na-MMT/PEI-*g*-PMMA films had a smooth and compact surface while Na-MMT dispersed uniformly on the fracture surface of the modified films. The R_a values of NRL films decreased with increasing addition amounts of Na-MMT/PEI-*g*-PMMA which prevented the migration of the protein and filled up the pits. The results of SEM and AFM indicated the good compatibility between NRL and exfoliated Na-MMT/PEI-*g*-PMMA particles. Tensile strength of NRL/Na-MMT/PEI-*g*-PMMA films increased to the maximum value with 10phr Na-MMT/PEI-*g*-PMMA when Na-MMT content was up to 3 wt %. All these results suggested that Na-MMT/PEI-*g*-PMMA latex would be useful for the modification of NRL gloves.

ACKNOWLEDGMENTS

This research was supported by the Fundamental Research Funds for the Central Universities (22A201514002).

REFERENCES

1. Nawamawat, K.; Sakdapipanich, J. T.; Ho, C. C.; Ma, Y.; Song, J.; Vancso, J. G. *Colloids Surf. A* **2011**, *390*, 157.
2. Sun, J.; Tian, X.; Feng, P.; Gong, S.; Yuan, Y. *J. Appl. Polym. Sci.* **2013**, *129*, 2404.
3. Arpornwichanop, T.; Polpanich, D.; Thiramanas, R.; Suteewong, T.; Tangboriboonrat, P. *Int. J. Biol. Macromol.* **2015**, *81*, 151.
4. Mitra, S.; Chattopadhyay, S.; Bhowmick, A. K. *J. Appl. Polym. Sci.* **2010**, *118*, 81.
5. Jacob, A.; Kurian, P.; Aprem, A. S. *J. Appl. Polym. Sci.* **2008**, *108*, 2623.
6. Usuki, A.; Kojima, Y.; Kawasumi, M.; Okada, A.; Fukushima, Y.; Kurauchi, T.; Kamigaito, O. *J. Mater. Res.* **1993**, *8*, 1179.
7. Kojima, Y.; Usuki, A.; Kawasumi, M.; Okada, A.; Fukushima, Y.; Kurauchi, T.; Kamigaito, O. *J. Mater. Res.* **1993**, *8*, 1185.
8. Lin, K. F.; Lin, S. C.; Chien, A. T.; Hsieh, C. C.; Yen, M. H.; Lee, C. H.; Lin, C. S.; Chiu, W. Y.; Lee, Y. H. *J. Polym. Sci. Part A: Polym. Chem.* **2006**, *44*, 5572.
9. Xu, M.; Choi, Y. S.; Hyun, W. K.; Hyun, K. J.; Jae, C. I. *Macromol. Res.* **2003**, *11*, 410.
10. Messersmith, P. B.; Giannelis, E. P. *J. Polym. Sci. Part A: Polym. Chem.* **1995**, *33*, 1047.
11. Hrachová, J.; Komadel, P.; Jochec-Mošková, D.; Krajči, J.; Janigová, I.; Šlouf, M.; Chodák, I. *J. Appl. Polym. Sci.* **2013**, *127*, 3447.
12. Lee, H. T.; Hwang, J. J.; Liu, H. J. *J. Polym. Sci. Part A: Polym. Chem.* **2006**, *44*, 5801.
13. Gu, Z.; Song, G.; Liu, W.; Wang, B.; Li, J. *Appl. Clay Sci.* **2009**, *45*, 50.
14. Darder, M.; Colilla, M.; Ruiz-Hitzky, E. *Chem. Mater.* **2003**, *15*, 3774.
15. Choi, Y. S.; Chung, I. J. *Polymer* **2004**, *45*, 3827.
16. Choi, Y. S.; Ham, H. T.; Chung, I. J. *Polymer* **2003**, *44*, 8147.
17. Chien, A. T.; Lin, K. F. *J. Polym. Sci. Part A: Polym. Chem.* **2007**, *45*, 5583.
18. Amarasiri, A.; Ratnayake, U. N.; De Silva, U. K.; Walpalage, S.; Siriwardene, S. *J. Natl. Sci. Found. Sri.* **2013**, *41*, 293.
19. Bhanvase, B. A.; Pinjari, D. V.; Gogate, P. R.; Sonawane, S. H.; Pandit, A. B. *Chem. Eng. J.* **2012**, *181*, 770.
20. Xu, M.; Choi, Y. S.; Wang, K. H.; Kim, J. H.; Chung, I. *J. Macromol. Res.* **2003**, *11*, 410.
21. Choi, Y. S.; Chung, I. J. *Macromol. Res.* **2003**, *11*, 425.
22. Choi, Y. S.; Choi, M. H.; Wang, K. H.; Kim, S. O.; Kim, Y. K.; Chung, I. J. *Macromolecules* **2001**, *34*, 8978.
23. Li, P.; Zhu, J.; Sunintaboon, P.; Harris, F. W. *J. Dispersion Sci. Technol.* **2003**, *24*, 607.
24. Wu, A.; Jia, J.; Luan, S. *Colloids Surf. A* **2011**, *384*, 180.
25. Li, P.; Zhu, J.; Sunintaboon, P.; Harris, F. W. *Langmuir* **2002**, *18*, 8641.
26. Sunintaboon, P.; Duangphet, S.; Tangboriboonrat, P. *Colloids Surf. A* **2009**, *350*, 114.
27. Lin, K. J.; Dai, C. A.; Lin, K. F. *J. Polym. Sci. Part A: Polym. Chem.* **2009**, *47*, 459.
28. Pavlidou, S.; Papaspyrides, C. D. *Prog. Polym. Sci.* **2008**, *33*, 1119.
29. Lin, K. J.; Lee, C. H.; Lin, K. F. *J. Polym. Sci. Part B: Polym. Phys.* **2010**, *48*, 1064.
30. Mathew, S.; Varghese, S. *J. Rubber Res.* **2005**, *8*, 1.